Stabilizing Quantum EMT on Noisy Hardware Using Multidimensional Richardson Extrapolation

Sijia Yu, Yifan Zhou
Department of Electrical and Computer Engineering
Stony Brook University, Stony Brook, NY, USA
{yu.sijia, yifan.zhou.1}@stonybrook.edu

Bin Wang, Qiang Zhang, Xiaochuan Luo, Tongxin Zheng
ISO New England Inc.
Holyoke, MA, USA
{bwang, qzhang, xluo, tzheng}@iso-ne.com

***Abstract*—Electromagnetic transient (EMT) simulations are essential for IBR-rich power grids. Quantum EMT (QEMT) leverages quantum computing to solve core EMT equations, offering the potential for superpolynomial performance enhancements. Yet, quantum algorithms inevitably suffer from hardware noise and circuit-level imperfections, introducing non-negligible inaccuracies into QEMT simulations. This paper develops a Richardson-extrapolation-enhanced quantum error mitigation framework for QEMT that jointly addresses multiple error sources. Our contributions include: 1) an in-depth analysis of quantum-induced inaccuracies in QEMT simulation; 2) a multidimensional Richardson extrapolation (RE)–based error-mitigation strategy tailored to QEMT; and 3) a superposition-enhanced RE strategy to mitigate quantum errors across multiple EMT equations simultaneously. Extensive case studies across varying system sizes, circuit depths, and noise levels demonstrate the effectiveness and practicality of the developed method in mitigating multiple errors jointly in QEMT simulation.**

***Index Terms*—Quantum electromagnetic transient (QEMT) simulation, EMT simulation, quantum error mitigation, Richardson extrapolation, quantum superposition.**

I. Introduction

EMT simulation is a foundational tool for analyzing fast transients and wide-band oscillations in modern power systems [1], but is well known for its high computational burden. As EMT studies have become routine requirements for the interconnection of inverter-based resources (IBRs), new generation resources, and large loads [2], achieving efficient EMT simulation has become critically important.

Substantial progress has been made in accelerating EMT from a classical computing perspective, including sparse computing, network segmentation, parallel computing [3], shifted frequency analysis [4], and semi-analytical frameworks [5]. Quantum EMT (QEMT) offers a fundamentally different angle by leveraging quantum mechanisms for acceleration. In the authors' prior work [6], [7], [8], QEMT employs quantum linear solvers to solve large-scale network nodal equations and has been successfully validated on the IEEE 906-bus grid using IBM's real quantum hardware. Related efforts such as [9] have further extended QEMT to handle switching devices, demonstrating its potential for analyzing complex IBR-dominated grids.

This work was supported in part by the Department of Navy award N000142512374 issued by the Office of Naval Research and in part by the National Science Foundation under Grant No. 2432387.

While promising, a major challenge associated with QEMT lies in the limitations of current quantum computers. Today's quantum hardware suffers from non-negligible noise, decoherence, and gate infidelities. These hardware imperfections can degrade circuit accuracy, potentially hindering stable EMT simulations when implemented directly on quantum devices. In existing studies, such errors are mitigated by incorporating additional classical iterations into the QEMT loop [6], [7], [8], [9], which inevitably incurs classical computing overhead. In the quantum community, various quantum error mitigation techniques have been developed [10]; however, their effectiveness and configurations for QEMT remain unexplored.

Moreover, QEMT depends on quantum circuits to perform computations, and it retrieves EMT solutions through quantum measurements. This workflow is fundamentally different from classical EMT procedures. It also remains unclear and uninvestigated whether these quantum-specific processes introduce additional inaccuracies into QEMT results.

This paper systematically studies quantum-induced errors in the QEMT pipeline. Our contributions are:

- We perform an in-depth analysis of quantum-induced inaccuracies in QEMT simulations, arising from both noisy quantum hardware and quantum circuit imperfections (including matrix encoding, quantum linear solver implementation, and measurement processes, which are often overlooked). Our analysis shows that the depth-dependent biases induced by these error sources can reinforce one another in QEMT simulation, jointly degrading solution accuracy.
- We develop a multidimensional Richardson extrapolation (RE)–based error mitigation strategy to simultaneously suppress multiple quantum error sources in QEMT. We demonstrate that, while RE can be numerically ill-conditioned under extremely small bias coefficients, realistic quantum hardware noise effectively amplifies the biases, making the extrapolation more stable and enabling effective mitigation of both hardware noise and circuit-level imperfections.
- We further develop a superposition-enhanced RE strategy to mitigate quantum errors across multiple EMT equations simultaneously without incurring additional circuit depth or measurement overhead.

Case studies across different system sizes and noise settings validate the effectiveness of the developed method, which offer

979-8-3315-8138-1

insights for designing more reliable and noise-robust quantum-enabled grid analytics on near-term quantum hardware.

II. Analysis of Quantum-Induced Errors in QEMT

A. Preliminaries of Classical and Quantum EMT

Classical EMT models each dynamic element as an equivalent conductance g and history current $i_{\mathrm{h}}(t)$ so that:

$$i(t) = gv(t) - i_{\mathrm{h}}(t) \tag{1}$$

and assembles all elements into the nodal equation:

$$\tilde{G}\, v_{\text{nodal}}(t) = i_{\text{nodal}}(t) \tag{2}$$

where $\tilde{G}$ is the network conductance matrix, $v_{\text{nodal}}(t)$ is the nodal voltage vector, and $i_{\text{nodal}}(t)$ is the total current injection, including both source injections and history currents. At each time step, EMT solves this N-dimensional network equation.

QEMT embeds the nodal equation into the quantum space using $n = \lceil \log_2 N \rceil$ qubits:

$$G\,|v_{\mathrm{Q}}\rangle = |i_{\mathrm{Q}}\rangle \tag{3}$$

where G pads $\tilde{G}$ into an $2^n \times 2^n$ Hermitian matrix as needed; $|i_{\mathrm{Q}}\rangle$ and $|v_{\mathrm{Q}}\rangle$ are quantum states corresponding to i and v.

Solving (3) generally involves three steps:

1) Encoding: The classical matrix G must first be represented by quantum operators. A common approach is to decompose G into a linear combination of unitaries (LCU):

$$G \xrightarrow{\text{encoding}} \sum\nolimits_j \alpha_j U_j^{\mathrm{E}} \tag{4}$$

where each U_j is a basis quantum operator that can be directly implemented on quantum hardware; superscript E represents operators in the encoding block.

2) Quantum linear solver (QLS) construction: A quantum circuit is then constructed to produce the solution state:

$$|v_{\mathrm{Q}}\rangle = \prod\nolimits_j U_j^{\mathrm{QLS}}\, |0\rangle^{\otimes n} \tag{5}$$

where $|0\rangle$ is the initial quantum state, and basis quantum operators U_j^{QLS} construct the quantum circuit associated with the chosen quantum linear solver (e.g., QFT-based operations in HHL [6] or a trained variational ansatz in VQLS [7]).

3) Measurement: Finally, measurements are performed on $|v_{\mathrm{Q}}\rangle$ to obtain the classical solution vector:

$$|v_{\mathrm{Q}}\rangle \xrightarrow{\text{measurement}} v_{\mathrm{Q}} \tag{6}$$

B. Quantum-Induced Error Sources in QEMT

In practice, each of the aforementioned steps suffer from various quantum-induced inaccuracies:

1) Embedding errors caused by decomposition: LCU decomposition is generally nontrivial and can produce thousands of terms for practical-scale matrices. Consequently, practical implementations often retain only the dominant components of the combination, which naturally induces truncation errors:

$$G \approx G_{\mathrm{LCU}} = \sum\nolimits_j \alpha_j U_j \tag{7}$$

2) Errors caused by unitary implementation: Even when implementing unitary operators on ideal quantum environments, there will be imperfections due to rounding errors [11]:

$$\Delta U_* := \widetilde{U}_* - U_* \tag{8}$$

where $\widetilde{U}_*$ is the actual implemented (imperfect) quantum operator. A large-scale grid may require thousands of unitary operators in the QEMT circuit; thus, the unitary implementation errors accumulate, leading to slight deviations in both QEMT encoding and QEMT quantum linear solver:

$$\Delta U^{\mathrm{LCU}} = \sum\nolimits_j \alpha_j \Delta U_j^{\mathrm{LCU}}\ ,\ \Delta U^{\mathrm{QLS}} = \prod\nolimits_j \Delta U_j^{\mathrm{QLS}} \tag{9}$$

3) Errors caused by QLS design: Moreover, QLSs are inherently approximate because they implement G^{-1} only through algorithmic approximations. VQLS is limited by variational optimization and offers no guarantee of convergence to the exact solution. HHL relies on repeated phase estimation (via QFT and inverse QFT) and terminates once a preset accuracy is met, which also has a residual error.

4) Errors caused by practical implementation: In addition, quantum device noise (e.g., gate and decoherence errors) accumulates with circuit depth and directly distorts the implemented unitary, so the prepared state deviates from the ideal one even before measurement. What's worse, measurement noise and finite-shot sampling further introduce stochastic errors in the estimated observables by introducing non-bias variances, while readout errors can create a systematic bias in the measured expectation values. In contrast,

C. Quantitative Impacts of Quantum-Induced Errors

All the aforementioned factors cause the QEMT output v_{Q} from (6) to deviate from the true classical EMT solution. In our prior work, we did not distinguish between the different error sources and all errors were addressed collectively through a classical iteration process, where the QLS is invoked repeatedly until convergence:

$$v_{\mathrm{Q}} \to G\,|\Delta v_{\mathrm{Q}}\rangle = |i_{\mathrm{Q}} - Gv_{\mathrm{Q}}\rangle \to v_{\mathrm{Q}} = v_{\mathrm{Q}} + \eta \Delta v_{\mathrm{Q}} \tag{10}$$

However, this introduces additional overhead in both classical computation and quantum circuit execution.

Therefore, the following analyzes the individual and combined impacts of these error sources, which will inspire a quantum-native error-mitigation strategy in Section III.

The output of the QEMT circuit is an implicit function of G; denote this mapping as $F(G)$. Denote the LCU-induced error in (7) as $\Delta G = G - G_{\mathrm{LCU}}$. Thus, the individual impact of ΔG on the QEMT output follows the Taylor expansion:

$$\begin{aligned} F(\Delta G) = F(G) &+ \langle \nabla_G F(G),\, \Delta G \rangle \\ &+ \tfrac{1}{2}(\Delta G)^{\top} H_{GG}\, \Delta G + O\big(\|\Delta G\|^3\big) \end{aligned} \tag{11}$$

where ∇ and H denote the first- and second-order derivatives.

979-8-3315-8138-1

Further, consider the unitary implementation error discussed in (9), its joint impact with ΔG is:

$$\begin{aligned} &F(\Delta G, \Delta U^{\mathrm{LCU}}) = F(G) + \langle \nabla_G F(G),\, \Delta G \rangle \\ &+ \langle \nabla_U F(G),\, \Delta U^{\mathrm{LCU}} \rangle \\ &+ \tfrac{1}{2}(\Delta U^{\mathrm{LCU}})^\top H_{UU}\, \Delta U^{\mathrm{LCU}} + (\Delta G)^\top H_{GU}\, \Delta U^{\mathrm{LCU}} \\ &+ \tfrac{1}{2}(\Delta G)^\top H_{GG}\, \Delta G + O\big(\|\Delta G\|^3, \|\Delta U^{\mathrm{LCU}}\|^3\big) \end{aligned} \tag{12}$$

which exhibits a bias caused by both sources. In other words, one error source can amplify the other one by introducing more joint noisy terms compared to equation (11). This similarly applies to the other quantum-induced noises and degrades the final solution accuracy.

Meanwhile, since each individual error is relatively small, their combined impact can be approximated by low-order polynomials or similarly analytical forms. This motivates the use of Richardson extrapolation for error mitigation.

III. Richardson Extrapolation-based QEMT Error Mitigation

Richardson extrapolation is a classical extrapolation technique widely adopted in quantum error mitigation methods such as zero-noise extrapolation (RE) [12], [13]. Its core idea is to run a quantum circuit at different noise levels, model the circuit output (e.g., expectations) as a function of the noise level, and then extrapolate this function to the zero-noise level to obtain the ideal (noise-free) solutions.

Although RE was originally designed to mitigate hardware noise, the analyses in (11) and (12) suggest that it can also address multiple quantum-induced errors. Thus, in this section, we develop a multidimensional Richardson extrapolation-based error mitigation strategy for QEMT and analyze its effectiveness in simultaneously handling multiple errors and multiple QEMT equations.

A. RE Expression for Single Error Source

Consider a single error source with noise strength parameter $\mu \in [0, 1]$. $\mu = 1$ corresponds to the actually implemented circuit. Analogous to (11), QEMT output can be expressed as:

$$F(\mu) = F(0) + \beta_1 \mu + \beta_2 \mu^2 + ... + O(\mu^K) \tag{13}$$

where β denotes the expansion coefficients.

The goal is to get $F(0)$, the noise-free output of QEMT. For a given G and a fixed circuit setup, the noisy behavior of the circuit is determined, meaning that β is theoretically constant. However, both β and $F(0)$. Thus, $F(0)$ will be inferred from noisy measurements.

A K-point Richardson estimator aims to form a linear combination of the noisy evaluations $F(\mu)$ at different noise levels, so that only $F(0)$ (i.e., the noise-free solution) and high-order noise (i.e., $O(\mu^K)$ which are negligible) remain [12]. Specifically, evaluate $F(\mu)$ at multiple noise levels $\mu_k = s_k \mu$ with scale factors $1 = s_0 < s_1 < \cdots < s_{K-1}$ (this is implemented by circuit folding [13]). According to (13), each evaluation satisfies:

$$\begin{aligned} F(\mu_k) = F(0) + \beta_1 s_k \mu + \beta_2 s_k^2 \mu^2 + ... + O(\mu^K), \\ k = 0, \ldots, K-1. \end{aligned} \tag{14}$$

Under proper selection of coefficients $\{w_k\}$, low-order noise terms in (14) can be eliminated to yield:

$$\begin{aligned} \widehat{F}_{\mathrm{RE}}(\mu) = F(0) + O(\mu^K) &:= \sum\nolimits_{k=0}^{K-1} w_k F(\mu_k) \\ &= \sum w_k F(0) + \sum \beta_1 w_k s_k \mu + ... + O(\mu^K) \end{aligned} \tag{15}$$

Consequently, $\{w_k\}$ should satisfy:

$$\sum\nolimits_k w_k = 1, \;\; \sum\nolimits_k w_k s_k = 0, \;\; \sum\nolimits_k w_k s_k^2 = 0, \;\; \cdots \tag{16}$$

B. Multidimensional RE for Joint Error Mitigation

If only a single error source is considered and its strength $\mu$is too small, the RE-corrected estimate may be dominated by sampling noise rather than the true bias, leading to inaccurate inference. Correspondingly, we develop a multidimensional RE to jointly eliminate multiple error sources.

Without loss of generality, we derive the method for the two-dimensional case, while it extends naturally to higher-dimensional error sources. Let $\mu \in [0, 1]$ and $\lambda \in [0, 1]$ denote two error resources (with (0,0) an ideal simulator and (1,1) the physical backend). A Taylor expansion around the ideal point $(\mu, \lambda) = (0, 0)$ yields:

$$F(\mu, \lambda) = F(0, 0) + \alpha_1 \mu + \beta_1 \lambda + O(\mu^2, \lambda^2, \mu\lambda^2) \tag{17}$$

Due to the reason that both μ and λ are depth dependent, performing the circuit folding with scale factors $s_k > 1$ leads to noise levels $(\mu, \lambda) \longrightarrow (s_k \mu,\, s_k \lambda)$. The corresponding QEMT output becomes:

$$\begin{aligned} F_k :=& F(s_k\mu, s_k\lambda) = F(0,0) + \alpha_{1,0} s_k \mu + \alpha_{0,1} s_k \lambda \\ &+ \alpha_{2,0}(s_k\mu)^2 + \alpha_{1,1}(s_k\mu)(s_k\lambda) + \alpha_{0,2}(s_k\lambda)^2 \\ &+ ... + O(\mu^j \lambda^{K-j}) \end{aligned} \tag{18}$$

for $k = 0, \ldots, K-1$ with $s_0 = 1$. By rewriting F_k as a function of s_k, it can be seen that:

$$\begin{aligned} F_k =& F(0,0) + s_k(\alpha_{1,0}\mu + \alpha_{0,1}\lambda) \\ &+ s_k^2(\alpha_{2,0}\mu^2 + \alpha_{1,1}\mu\lambda + \alpha_{0,2}\lambda^2) \\ &+ ... + O(\mu^j \lambda^{K-j}) \end{aligned} \tag{19}$$

In analogy with (15), the multidimensional Richardson estimator, thus, requires the following to eliminate the low-order noise terms:

$$\widehat{F}_{\mathrm{RE}} := \sum\nolimits_{k=0}^{K-1} w_k F_k = F(0,0) + O(\mu^j \lambda^{K-j}) \tag{20}$$

with weights $\{w_k\}$ chosen to satisfy:

$$\sum\nolimits_k w_k = 1, \;\; \sum\nolimits_k w_k s_k = 0, \;\; \sum_k w_k s_k^2 = 0, \;\; \cdots \tag{21}$$

Consequently, after solving $\{w_k\}$, the noise-free solution $F(0, 0)$ can be resolved from (20) as each F_k is pre-evaluated through circuit folding.

Notably, (18) shows that with multiple noise sources, the noise slope is no longer controlled by any single noise term, but by the combined depth-dependent contribution from multiple noises. This makes the values $F(s_k\mu, s_k\lambda)$ more widely separated as s_k increases, making the slope of F

979-8-3315-8138-1

with respect to depth easier to resolve. Consequently, the Richardson system for $\{w_k\}$ is better conditioned and more numerically stable for suppressing quantum-induced noises.

C. *Superposition-Enhanced RE for Batch QEMT Solver*

Further, a superposition-enhanced RE will handle errors in multiple QEMT equations at the same time.

1) Basis-and-batch QEMT solver: One practical challenge in the QEMT measurement process (6) is that quantum circuits return probability amplitudes, not the actual value of v. To overcome this, our prior work developed a *basis-and-batch QEMT solver* [7]:

$$Gv_k = i_k,\;\; k = 1, \dots, N. \implies (I_n \otimes G)\, V_{\text{all}} = I_{\text{all}} \tag{22}$$

As shown, in the basis stage, each QEMT equation only formulates the solution under a basis quantum state i_k; this ensures that measurement outcomes are strictly nonnegative and therefore directly recoverable from the probability amplitudes. Then, in the batch stage, the N basis QEMT equations are stacked and solved together as a single large linear system, yielding the full solution vector.

2) Superposition-enhanced RE: We will show that RE naturally applies to this batch QEMT solver by leveraging quantum superposition, and introduces only minimal additional circuit construction or measurement effort.

Based on (22), the batch QEMT is expected to realize the following function:

$$V_{\text{all}} = (I_n \otimes G)^{-1} I_{\text{all}} = (I_n \otimes G^{-1}) I_{\text{all}} \tag{23}$$

Correspondingly, its quantum circuit can be constructed as:

$$U^{BQLS} = U_{I_n \otimes G^{-1}} U_{|I_{\text{all}}\rangle} |0\rangle = I_n \otimes U_{G^{-1}} U_{|I_{\text{all}}\rangle} |0\rangle \tag{24}$$

Both $U_{I_n \otimes G^{-1}}$ and $U_{|e\rangle} = U_{|I_{\text{all}}\rangle|0\rangle}$ are implemented using two registers: an index register and a data register.

For $U_{I_n \otimes G^{-1}}$, note that:

$$U_{I_n \otimes G^{-1}} = I_n \otimes U_{G^{-1}} \tag{25}$$

The index register remains idle while the data register executes $U_{G^{-1}}$, i.e., re-uses the matrix inversion block in the original QEMT circuit, which is of the same circuit depth and incurs no efforts for rebuilding quantum circuits.

For $U_{|e\rangle}$, its construction incurs only an $O(\log N)$ overhead: specifically, $\log N$ Hadamard gates on the index register and $\log N$ CNOT gates from the index register to the data register. Thus, the dominant circuit depth continues to arise from implementing G^{-1} on the data register, matching the depth of the non-batch configuration. This preserves the key advantages of applying the RE method, including:

- Smaller folding and sampling overhead: For a given quantum device, a shallower circuit suffers less from depth-dependent quantum noise. In other words, the higher-order noise terms in (13) will contribute significantly less. This enables using moderate noise scales s, thus reducing the number of circuit implementations and shots, to achieve an expected accuracy of extrapolation.
- Smaller variance and more reliable extrapolation performance: Compared with a generic QLS circuit for solving a matrix of the same size as $I_n \otimes G$, the block-structured circuit for $I_n \otimes G^{-1}$ is much shallower, leading to a smaller per-sample variance $\mathrm{Var}[F(s_i)]$. Consequently, the bias-induced slope between $F(s_i)$ and $F(s_j)$ is less likely to be obscured by noise, allowing reliable extrapolation with moderate noise scales and circuit folds.

Remarks: Yet, a natural limitation of RE is its sensitivity to circuit depth. RE assumes a small-error expansion (e.g., (13) and (17)), which is only valid when the effective noise scale $s\mu$ is modest. For deep circuits, large $s\mu$ breaks this approximation, and the folded circuits required by RE become too noisy. In this work, the QEMT circuit is implemented using variational quantum linear solvers (VQLS), which naturally leads to shallow quantum circuits. Yet, the applicability of RE to QLS that may require substantially deeper circuits (e.g., HHL) will need future investigation.

IV. Case Study

This section validates the effectiveness of RE for a more reliable QEMT implementation in noisy quantum environments and analyzes its impact factors. All simulations are implemented with IBM Quantum Hub.

A. *Effectiveness of RE in QEMT*

The RE-enhanced QEMT trajectories for the IEEE 123-bus test feeder are shown in Fig. 1. The node-voltage closely track the EMTP results over the entire simulation horizon under both nominal conditions and fault conditions.

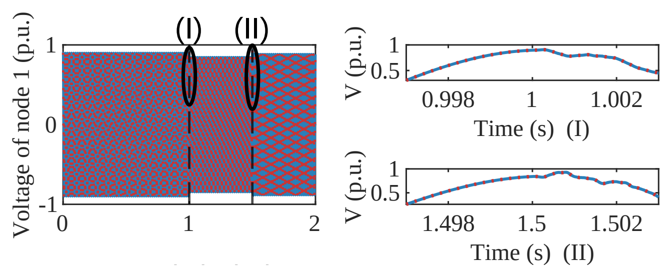

Fig. 1. RE-enhanced QEMT (purple lines) on the IEEE 123-bus test feeder compared to classical EMT results (blue lines) under a short-circuit fault.

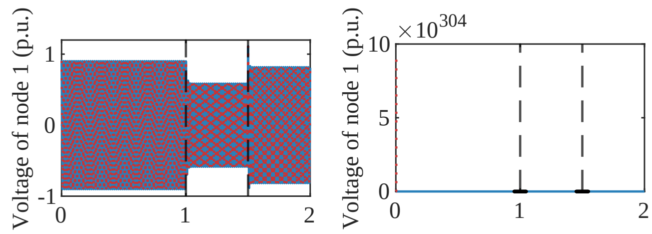

Fig. 2. Comparison between QEMT with (left) and without RE (right) in the IEEE 13-bus test feeder. The classical iteration number is limited to 2.

Yet, one may note that in our previous study [7], the raw QEMT algorithm without RE also produced accurate EMT solutions. This is primarily because the classical iteration performs error compensation (see (10)) to mitigate quantum-induced errors (resulting in extra classical overheads). To more directly demonstrate the benefit of incorporating RE, Fig 2

979-8-3315-8138-1

shows the results with the classical iteration count limited to 2. It can be seen that QEMT fails to converge on noisy hardware even for the small IEEE 13-bus grid when a fault occurs at 1s; whereas with the RE strategy, the QEMT simulation converges reliably despite quantum noise.

Further, Table I presents the number of classical iterations required under different settings. In both ideal quantum simulators (noise-free) and real, noisy quantum hardware, RE substantially reduces the error of a single quantum circuit and, thus, significantly reduces the number of classical iterations. This indicates that quantum-induced errors are mitigated more directly at the quantum circuit level, rather than relying heavily on classical modules. Specifically, by comparing the "noisy + RE" setting and the "noise-free" baseline, it can be seen that even without quantum hardware noise, other types of quantum-induced noise still prevent the QLS from achieving perfect accuracy, thereby still requiring classical iterations. In contrast, incorporating RE effectively removes multiple types of quantum-induced errors, leading to higher circuit-level accuracy (and a smaller number of iterations), which even slightly outperforms that of the noise-free simulator.

TABLE I. Classical iteration counts for different IEEE test systems under different noise and error correction settings.

System	Case	Error[1]	Iteration[2]
4–bus	noise–free	0.000321	3
	noise–free + RE	0	2
	noisy	0.031636	8
	noisy + RE	0.00001	2
13–bus	noise–free	0.00849	4
	noise–free + RE	0.00007	4
	noisy	0.31646	11
	noisy + RE	0.00002	4
123–bus	noise–free	0.000145	4
	noise–free + RE	0	4
	noisy	0.31634	18
	noisy + RE	0.00004	4

[1] "Error" measures the accuracy of the U^{LCU} block built for (4).
[2] "Iteration" counts how many classical iterations are needed for (10).

B. Impact Factor Analysis of RE

Table II further studies the impact factors of RE performance. When the circuit depth L increases, the error without RE grows, whereas the RE-corrected error remains small and can even decrease under moderate noise. When the noise scale increases, the RE performance may degrade as the samples used for extrapolation are too noisy to yield a trustworthy zero-noise estimate, as discussed in Section III.

V. Conclusions

This paper develops a Richardson-extrapolation–enhanced QEMT simulation approach for more reliable and stable performance on noisy quantum hardware. By analyzing the entire QEMT pipeline, we show how LCU-based matrix approximation, circuit imperfections, and depth-dependent device noise jointly bias EMT solutions. We then develop a multidimensional RE method to suppress these errors simultaneously.

TABLE II. Impact of circuit depth and noise scale on RE performance.

Parameter	Error (no RE)	Error (with RE)	Change (%)
Impact of circuit layer L			
$L=2$	0.077	0.00403	94.8
$L=3$	0.0446	0.000046	99.9
$L=4$	0.0529	0.000102	99.8
Impact of noise scale s_k			
$[1,3]$	0.0665	0.000257	99.6
$[11:2:15]$	0.0665	0.00134	98.0
$[23:2:27]$	0.0665	0.00775	88.3

Case studies on typical IEEE testing grids show that the RE-enhanced QEMT markedly reduces the error of the QEMT circuit's output, and accordingly, reduces the number of iterations needed originally in the classical error compensation module in QEMT. These results indicate that RE-based mitigation is a practical building block for scalable, noise-robust quantum grid analytics in the NISQ era and is readily extensible to other quantum-enabled power grid applications such as quantum power flow and state estimation.

References

[1] S. Filizadeh, J. Belanger, F. Fernandez, P. Forsyth, J. Mahseredjian, J. Morales, and G. Lietz, "Electromagnetic transient modeling and simulation of large power systems: EMT simulators for the future grid [feature]," *IEEE Power and Energy Magazine*, vol. 23, no. 4, pp. 53–65, 2025.

[2] North American Electric Reliability Corporation, "Reliability Guideline: Electromagnetic Transient Modeling for BPS-Connected Inverter-Based Resources—Recommended Model Requirements and Verification Practices," tech. rep., North American Electric Reliability Corporation, 2023.

[3] M. Xiong, B. Wang, D. Vaidhynathan, J. Maack, M. J. Reynolds, A. Hoke, K. Sun, D. Ramasubramanian, V. Verma, and J. Tan, "An open-source parallel EMT simulation framework," tech. rep., National Renewable Energy Laboratory (NREL), Golden, CO (United States), 2023.

[4] P. Zhang, J. R. Martí, and H. W. Dommel, "Shifted-frequency analysis for EMTP simulation of power-system dynamics," *IEEE Transactions on Circuits and Systems I: Regular Papers*, vol. 57, no. 9, pp. 2564–2574, 2010.

[5] H. Cui, F. Li, and K. Tomsovic, "Hybrid symbolic-numeric framework for power system modeling and analysis," *IEEE Transactions on Power Systems*, vol. 36, no. 2, pp. 1373–1384, 2020.

[6] Y. Zhou, F. Feng, and P. Zhang, "Quantum electromagnetic transients program," *IEEE Transactions on Power Systems*, vol. 36, no. 4, pp. 3813–3816, 2021.

[7] Y. Zhou, P. Zhang, and F. Feng, "Noisy-intermediate-scale quantum electromagnetic transients program," *IEEE Transactions on Power Systems*, vol. 38, no. 2, pp. 1558–1571, 2022.

[8] S. Yu and Y. Zhou, "Quantum shifted frequency analysis through Krylov subspace decomposition," in *2025 IEEE Power & Energy Society General Meeting (PESGM)*, pp. 1–5, IEEE, 2025.

[9] Q. Lou, Y. Xu, and W. Gu, "Matrix low-dimensional qubit casting based quantum electromagnetic transient network simulation program," *arXiv preprint arXiv:2502.11728*, 2025.

[10] Z. Cai, R. Babbush, S. C. Benjamin, S. Endo, W. J. Huggins, Y. Li, J. R. McClean, and T. E. O'Brien, "Quantum error mitigation," *Reviews of Modern Physics*, vol. 95, no. 4, p. 045005, 2023.

[11] J. Klamroth and B. Beckert, "Bounding rounding errors in the simulation of quantum circuits," in *2024 IEEE International Conference on Quantum Software (QSW)*, pp. 99–106, IEEE, 2024.

[12] M. Krebsbach, B. Trauzettel, and A. Calzona, "Optimization of richardson extrapolation for quantum error mitigation," *Physical Review A*, vol. 106, no. 6, p. 062436, 2022.

[13] A. C. Vazquez, R. Hiptmair, and S. Woerner, "Enhancing the quantum linear systems algorithm using richardson extrapolation," *ACM Transactions on Quantum Computing*, vol. 3, no. 1, pp. 1–37, 2022.

979-8-3315-8138-1